Applied Thermal Engineering 35 (2012) 145–156

Contents lists available at SciVerse ScienceDirect

Applied Thermal Engineering

journal homepage: www.elsevier.com/locate/apthermeng

Thermal analysis of mass concrete embedded with double-layer staggered heterogeneous cooling water pipes

Jian Yang [a,b], Yu Hu [a], Zheng Zuo [a], Feng Jin [a,*], Qingbin Li [a]

[a] State Key Laboratory of Hydroscience and Engineering, Tsinghua University, 100084 Beijing, China
[b] Clean Energy Research Institute, China Huaneng Group, 100098 Beijing, China

ARTICLE INFO

Article history:
Received 18 April 2011
Accepted 4 October 2011
Available online 19 October 2011

Keywords:
Mass concrete
Hydration heat
Cooling water pipe
Equivalent equation of heat conduction
Adiabatic temperature rise curve

ABSTRACT

Removal of hydration heat from mass concrete during construction is important for the quality and safety of concrete structures. In this study, a three-dimensional finite element program for thermal analysis of mass concrete embedded with double-layer staggered heterogeneous cooling water pipes was developed based on the equivalent equation of heat conduction including the effect of cooling water pipes and hydration heat of concrete. The cooling function of the double-layer staggered heterogeneous cooling pipes in a concrete slab was derived from the principle of equivalent cooling. To improve the applicability and precision of the equivalent heat conduction equation under small flow, the cooling function was revised according to its monotonicity and empirical formulas of single-phase forced-convection heat transfer in tube flow. Considering heat hydration of concrete at later age, a double exponential function was proposed to fit the adiabatic temperature rise curve of concrete. Subsequently, the temperature variation of concrete was obtained, and the outlet temperature of cooling water was estimated through the energy conservation principle. Comparing calculated results with actual measured data from a monolith of an arch dam in China, the numerical model was proven to be effective in sufficiently simulating accurate temperature variations of mass concrete.

1. Introduction

Mass concrete has been widely used in civil engineering, e.g. dam, building, and bridge construction, and is usually poured in large thin slabs. Due to the relatively small conductivity of concrete, little hydration heat diffuses from the surface during construction, so that internal temperature easily rises to exceed 70 °C. It may lead to thermal-stress-induced cracking and structural weakening [1,2]. Moreover, the next slab cannot be poured until the previous slab has been refrigerated to a prescribed temperature level, which often delays the construction process. Measures should be adopted to limit the temperature rise in mass concrete within an acceptable level [3]. In addition to the application of pre-cooling techniques (e.g. cooling aggregates and reducing cement content), post-cooling of in-place concrete by circulating a cool liquid (commonly cold water) through built-in thin-walled pipes for a considerable amount of time is also widely used. This post-cooling technique was first successfully employed during the construction of the Hoover dam [4]. Instead of using full air conditioning, the use of a hydronic system in multi-story office buildings where pipes embedded in the concrete slabs circulate cold or hot water in different seasons has been introduced [5].

The first solution to the problem of embedded cooling water pipes was proposed by the U.S. Bureau of Reclamation after the completion of the Hoover dam [6]. Provided that cooling pipes are arranged at regular spatial intervals, the concrete could be regarded as a series of unit cells with a pipe located at the cell center. Each unit cell can then be simplified as a long hollow circular cylinder with insulated outer boundary. Based on this assumption, the U.S. Bureau of Reclamation derived strict and approximate solutions to the two- and three-dimensional (3D) problem without an internal heat resource. Zhu [7] addressed the problem of heat resource. Above solutions remain effective guides for engineers in the design and operation of cooling pipe systems up to the present [3,8]. However, this approach is limited by its inability to account for different construction conditions, different thermal properties of concrete, and arbitrary time-dependent variations in conditions of cooling water.

Based on the periodic temperature field along pipe arrangement directions in mass concrete embedded in a rectangular pipe mesh, Liu [9] proposed an analytic model of temperature variation. Detailed descriptions of the principal aspects affecting the temperature field, including concrete and pipe material properties, pipe sizes, pipe spacing, and the cooling process, were presented. Charpin et al. [10] applied non-dimensional analysis to the problem of a pipe embedded

* Corresponding author. Tel.: +86 0 1062794242; fax: +86 0 1062782159.
E-mail addresses: yangkee@gmail.com (J. Yang), yu-hu@tsinghua.edu.cn (Y. Hu), jinfeng@tsinghua.edu.cn (F. Jin).

1359-4311/$ – see front matter © 2011 Elsevier Ltd. All rights reserved.
doi:10.1016/j.applthermaleng.2011.10.016

Nomenclature

b	parameter for equivalent material thermal diffusivity (Eq. (30))
c	specific heat (J/kg °C)
C_s	Stefan–Boltzman constant (5.669×10^{-8} W/m^2 °C^4)
d	inner diameter of cooling pipe (m)
e	emissivity of surface
f	friction factor
G_t	total amount of solar energy reaching the surface (W/m^2)
h	heat convection coefficient (W/m^2 °C)
h_r	linearized radiation coefficient (W/m^2 °C)
i	the layer number of insulator
k	thermal conductivity (W/m °C)
l	thickness of the heat insulator (m)
L	length of cooling pipe (m)
m	a parameter that represents the heat generation rate (1/day)
n	the normal to the surface
Nu	Nusselt number
Pr	Prandtl number
q	flow of cooling water (m^3/s)
q_a	absorbed solar radiation flux (W/m^2)
q_c	convective flux (W/m^2)
q_{cool}	heat absorbed by cooling water per unit time (W)
q_{m1}	turning point flow of cooling water (m^3/s)
q_{m2}	critical laminar flow of cooling water (m^3/s)
q_r	radiative flux (W/m^2)
q_s	a scale factor
Q	total internal heat source per unit volume (J/m^3)
$\dot{Q}$	the rate of total internal heat source per unit volume (W/m^3)
r	inner radius of the concrete cylinder (m)
r_0	outer radius of the cooling pipe (m)
R	outer radius of the concrete cylinder (m)
Re	Reynolds number
S	spatial interval of the cooling pipe (m)
t	time (s)
t_p	thickness of cooling pipe (m)
T	temperature (°C)
T_0	initial temperature of concrete
T_a	ambient air temperature (°C)
T_c	the concrete placing temperature (°C)
T_e	the deep earth temperature (°C)
T_m	mean temperature of concrete cylinder (°C)
$T_{w\text{-}in}$	inlet temperature of cooling water (°C)
$T_{w\text{-}out}$	outlet temperature of cooling water (°C)
u_m	mean velocity of flow (m/s)

Greek symbols

α	material thermal diffusivity (m^2/s)
α_1, α_2	parameters for adiabatic temperature rise curve of double exponential function (Chapter 4)
α'	equivalent material thermal diffusivity (m^2/s)
β	a parameter about the rectangular aspect ratio (Chapter 3.1)
Γ	the boundary surface
Γ_q	the exposed surface
ζ	solar absorptivity
θ	adiabatic temperature rise of concrete (°C)
θ_0	maximum temperature rise of concrete under adiabatic conditions (°C)
μ	dynamic viscosity (kg/m s)
ν	kinematic viscosity (m^2/s)
ξ	parameter for the cooling function
ρ	material's density (kg/m^3)
τ	time (s)
φ	cooling function
Δt	the time interval

Superscripts

n	step number
w	cooling water
p	cooling pipe
h	horizontal
v	vertical

in a long insulated cylindrical slab of concrete and reduced it to a one-dimensional heat equation. An analytic solution for the temperature rise along the pipe and within the concrete was then derived. Following this study, Myers et al. [11] developed a numerical procedure and discussed the effect of varying model parameters. However, the application of analytic methods in engineering remains limited because of its inconvenience and inflexibility.

Recently, finite element methods [12–15] have been developed and widely used in the thermal analysis of mass concrete with cooling pipe coils. Neglecting the temperature gradient at the direction of the cooling pipe, Zhu et al. [12] presented an iterative method to obtain the temperature field of the concrete and water. A series of cross sections with equidistance were taken in the direction perpendicular to the cooling pipe and the temperature field in each cross section was analyzed by two-dimensional finite element method. A refinable finite element mesh should be adopted near the pipe to ensure the accuracy of the solution. Kim et al. [13] implemented a line element for the modeling of pipe and applied internal flow theory for calculating temperature variations of cooling water. In this program, the requirement that the line element for modeling of pipe must be located at an edge of or run across a solid concrete element may lead to inconveniences in the model preprocessing and considerable computational cost. Therefore, these methods are not sufficiently efficient for thermal and stress analysis of large-scale concrete structures. To overcome this problem, Zhu [16] introduced the effect of the cooling pipe as a heat sink or as a negative heat source, and proposed an equivalent equation of heat conduction to calculate the temperature variation with the conventional finite element mesh. Although this is an approximation method, the application of the equivalent equation of heat conduction in practical engineering projects has been reported in previous literature [16,17]. To our best knowledge, these applications are concerned with a single cooling pipe material in concrete. Upon consideration of construction progress and cooling efficiency, the layout of double-layer staggered heterogeneous cooling pipes in a concrete slab was gradually adopted.

In this paper, we developed a 3D finite element procedure for thermal analysis of mass concrete with a pipe cooling system. The solution for the effect of double-layer staggered heterogeneous cooling pipes was derived from the concept of equivalent cooling. To improve the applicability and precision of the equivalent heat conduction equation under laminar flow condition, the cooling function was revised according to empirical formulas of single-phase forced-convection heat transfer in tube flow. Considering

heat contribution of other cementitious materials at later age, a double exponential function was proposed to fit the adiabatic temperature rise curve of concrete. Subsequently, the temperature variation of concrete was obtained and the outlet temperature of cooling water was estimated through the energy conservation principle. The reliability of the developed program was verified by a case study on a monolith of an arch dam in China.

2. Mathematical modelling

2.1. Equivalent equation of heat conduction

Considering that the material is isotropic and homogeneous and that its thermal properties are independent of temperature, heat transfer in a 3D solid region is governed by the following heat conduction equation [18]:

$$\frac{\partial T}{\partial t} = \alpha\left(\frac{\partial^2 T}{\partial x^2}+\frac{\partial^2 T}{\partial y^2}+\frac{\partial^2 T}{\partial z^2}\right) + \frac{\dot{Q}}{\rho c} \tag{1}$$

When there is no cooling system in mass concrete, the origin of the internal heat source comes solely from the hydration heat of concrete, which could be referred to as positive heat source $\dot{Q}^+$. With respect to cooling pipes embedded in mass concrete, this system performs as a heat sink to remove heat from concrete. Supposing that the cooling water is incompressible and that the thermal conductivity of cooling water is extremely small in the radial direction of a pipe, Zhu [16] suggested that heat removal by a cooling system could be regarded as negative heat source $\dot{Q}^-$ and is uniformly dispersed across the region where the cooling system is desired. The following equation is then derived:

$$\dot{Q} = \dot{Q}^+ + \dot{Q}^- \tag{2}$$

Consequently, the effect of cooling water pipes was implanted in the heat conduction equation. The solution of this method is the mean temperature in the domain, and the temperature gradient near the cooling pipes could not be obtained. In practice, when cooling water flows through the pipe and absorbs heat from the concrete, the temperature of water gradually rises along the pipe. This results in varying heat removal rates along the direction of flow. However, the flow direction is alternated at a fixed interval in most projects, usually no more than two days, which assures even trend of distribution of temperature field in the concrete. Thus, it is acceptable to uniformly disperse heat removal throughout the solution domain.

Without internal heat generation, the mean temperature of a concrete cylinder with cooling pipes is given by the following equation [6]:

$$T_m(t) = T_{w-in} + (T_0 - T_{w-in})\varphi(t) \tag{3}$$

where $\varphi(t)$ is the cooling function of the properties of concrete, pipes, and cooling water.

Generally, the adiabatic temperature rise of concrete is defined as:

$$\theta(t) = \theta_0 f(t) \tag{4}$$

The increment of adiabatic temperature rise of concrete at a certain time τ due to hydration heat is assumed as $(\partial\theta/\partial\tau)d\tau$. Considering the effect of a pipe cooling system, the temperature rise at end time t is modified as $\varphi(t-\tau)(\partial\theta/\partial\tau)d\tau$. Subsequently, the mean temperature of concrete with internal heat generation with respect to the cooling water pipes is the following integration equation:

$$T'(t) = \int_0^t \varphi(t-\tau)\frac{\partial\theta}{\partial\tau}d\tau = \theta_0\psi(t) \tag{5}$$

where $\psi(t)$ is a function of $\varphi(t)$ and $f(t)$. Thus, the total heat source, including heat generation and heat removal from the concrete, is derived as follows:

$$Q = \rho c[T_m(t) - T_0] + \rho c T'(t) \tag{6}$$

Plugging Eq. (6) into Eq. (1), the heat conduction equation can be rewritten as:

$$\frac{\partial T}{\partial t} = \alpha\left(\frac{\partial^2 T}{\partial x^2}+\frac{\partial^2 T}{\partial y^2}+\frac{\partial^2 T}{\partial z^2}\right) + (T_0 - T_{w-in})\frac{\partial\varphi}{\partial t} + \theta_0\frac{\partial\psi}{\partial t} \tag{7}$$

This is the equivalent equation of heat conduction including hydration heat of concrete and the effect of cooling water pipes.

2.2. Boundary conditions

For the thermal analysis of hydration heat in concrete structures with cooling water pipes, the semi-unbounded soil or rock foundation connected with the structure has to be truncated into a finite region. In the truncated structure-foundation solution domain, four types of boundary conditions should be determined (Fig. 1).

The exposed surfaces consist of the concrete-air interface Γ_1, where the temperature is influenced by convection heat transfer and radiation heat transfer, as well as solar radiation. The boundary condition at the concrete air interface Γ_1 can be expressed as:

$$-k\frac{\partial T}{\partial n} = q_c + q_r - q_a \tag{8}$$

Heat exchange by convection due to temperature differences between Γ_1 and ambient temperature is defined by Newton's cooling law:

$$q_c = h(T - T_a) \tag{9}$$

Heat exchange by electromagnetic radiation is given by the Stefan–Boltzmann law:

$$q_r = eC_s\left(T^4 - T_a^4\right) \tag{10}$$

This equation can be rewritten in linear form as:

$$q_r = h_r(T - T_a) \tag{11}$$

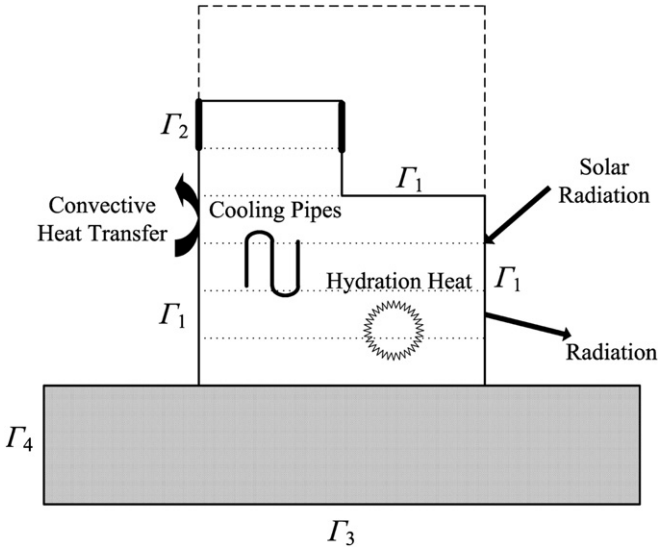

Fig. 1. Boundary conditions of thermal analysis of the structure-foundation system.

$$h_r = eC_s\left(T^2 + T_a^2\right)(T + T_a) \tag{12}$$

For simplicity, both convection and radiation heat transfer coefficients are usually combined to generate a comprehensive convection coefficient. The amount of absorbed solar radiation is given by

$$q_a = \zeta G_t \tag{13}$$

Covered surfaces Γ_2, which are covered by formworks or heat insulators during the construction phase, are the second type of boundary condition. In general, the boundary condition is still expressed as Eq. (8), but the convection coefficient of the covered surfaces should be modified as follows:

$$h_s = \frac{1}{(1/h) + \sum(l_i/k_i)} \tag{14}$$

In practice, the exposed and covered surfaces of concrete structures vary throughout the construction process. Thus, a certain surface is alternately exposed and covered during construction.

The horizontal boundary of the truncated foundation Γ_3 is usually a constant temperature:

$$T(\tau) = T_e \tag{15}$$

At the vertical surfaces of the truncated foundation Γ_4, the boundary condition is defined as

$$-k\frac{\partial T}{\partial n} = 0 \tag{16}$$

2.3. Finite element formulation of heat transfer

In this paper, the finite element discretization of Eq. (7) with implementation of the aforementioned boundary conditions results in:

$$[\mathbf{C}]\left\{\frac{\partial \mathbf{T}}{\partial t}\right\} + [\mathbf{K}]\{\mathbf{T}\} = \{\mathbf{F}\} \tag{17}$$

The matrices and vectors are defined as:

$$[\mathbf{C}] = \int_{\Omega} \rho c[\mathbf{N}]^{\mathrm{T}}[\mathbf{N}]d\Omega \tag{18}$$

$$[\mathbf{K}] = \int_{\Omega} [\mathbf{B}]^{\mathrm{T}}[\mathbf{D}][\mathbf{B}]d\Omega + \int_{\Gamma} h[\mathbf{N}]^{\mathrm{T}}[\mathbf{N}]d\Gamma \tag{19}$$

$$\{\mathbf{F}\} = \int_{\Omega} \dot{Q}[\mathbf{N}]^{T}d\Omega - \int_{\Gamma_q} q[\mathbf{N}]^{\mathrm{T}}\mathrm{d}\Gamma_q + \int_{\Gamma} hT_a[\mathbf{N}]^{\mathrm{T}}\mathrm{d}\Gamma \tag{20}$$

where $[\mathbf{N}] = [N_i, N_j, \ldots, N_r]$ is the matrix for shape function and $[\mathbf{B}]$ is the matrix for derivative of the shape function with respect to natural coordinates. Supposing k is independent of temperature, the backward difference method can be employed in the temporal discretization of Eq. (17), which leads to the following equation:

$$([\mathbf{C}] + [\mathbf{K}]\Delta t)\{\mathbf{T}\}^{n+1} = [\mathbf{C}]\{\mathbf{T}\}^{n} + \Delta t\{\mathbf{F}\}^{n+1} \tag{21}$$

Eq. (21) gives the nodal values of temperature at $n+1$ time level, which are calculated using the n time-level values of temperature and the forcing vector $\{\mathbf{F}\}$.

2.4. Initial conditions for the fresh concrete

The technique of element removal or reactivation is commonly employed for modeling the construction of concrete structures. When a fresh concrete slab is poured, the corresponding elements in the finite element model are immediately activated and included in the solution procedure. At this moment, the temperature of these nodes, by which the active elements are connected with preexisting elements, is equivalent to the computed temperature obtained from the previous step. However, the actual initial temperature of fresh concrete elements is their placing temperature. An accurate temperature solution for fresh concrete elements can only be solved by the following equation instead of Eq. (21) at the activation step:

$$([\mathbf{C}] + [\mathbf{K}]\Delta t)\{\mathbf{T}\}^{n+1} = [\mathbf{C}]\{\mathbf{T}_c\} + \Delta t\{\mathbf{F}\}^{n+1} \tag{22}$$

Compared with Eq. (21), Eq. (22) can be transformed to the following form:

$$([\mathbf{C}] + [\mathbf{K}]\Delta t)\{\mathbf{T}\}^{n+1} = [\mathbf{C}](\{\mathbf{T}_c\} + \{\mathbf{T}\}^{n} - \{\mathbf{T}\}^{n}) + \Delta t\{\mathbf{F}\}^{n+1} \tag{23}$$

The expression in Eq. (23) can be simplified to:

$$([\mathbf{C}] + [\mathbf{K}]\Delta t)\{\mathbf{T}\}^{n+1} = [\mathbf{C}]\{\mathbf{T}\}^{n} + \Delta t\{\mathbf{F}'\}^{n+1} \tag{24}$$

Where:

$$\{\mathbf{F}'\}^{n+1} = \{\mathbf{F}\}^{n+1} + \{\mathbf{f}\} \tag{25}$$

$$\{\mathbf{f}\} = \frac{1}{\Delta t}[\mathbf{C}](\{\mathbf{T}_c\} - \{\mathbf{T}\}^{n}) \tag{26}$$

Eq. (24) indicates that if a continuous accurate analysis without manual correction of nodal temperature is expected, an additional heat flux $\{\mathbf{f}\}$ must be forced to the fresh concrete elements at the activation step due to the difference in initial temperature between these elements and the poured ones. However, it is noticeable that except the boundary nodes in common with the mesh prior to element activation, the temperature of new activated nodes before being activated are always equal to the placing temperature. This fact implies the element of the additional heat flux vector $\{\mathbf{f}\}$ for most of new activated nodes is zero according to Eq. (26). And the element of the additional heat flux vector $\{\mathbf{f}\}$ for aforementioned boundary nodes is commonly negative since the concrete placing temperature is generally lower than that of the last step. Certainly the nonzero additional heat flux will affect neighbouring nodes due to heat conduction at the activation step.

3. Effect of cooling water pipes

3.1. General equations for effect of cooling water pipes

To solve the equivalent equation of heat conduction, Zhu [16,19] proposed the following formula for the cooling function $\varphi(t)$:

$$\varphi(t) = \exp\left[-k_1(zt)^s\right] \tag{27}$$

$$z = \frac{\alpha}{4R^2} \tag{28}$$

where $k_1 = 2.08 - 1.174\xi + 0.256\xi^2$ and $s = 0.971 + 0.1485\xi - 0.0445\xi^2$, as determined by fitting analysis using experimental information [16]; while $\xi = kL/c_w\rho_w q_w$ and $R = \sqrt{\beta S_h S_v/\pi}$. According to Stucky et al. [20], a rectangular unit cell with a rectangular aspect ratio contained between 1:1 and 1:2 behaves like a hexagon whose pipes should refrigerate a zone of action of 7% or greater. Thus, β is 1.0 and

1.07 for a hexagonal and rectangular pipe mesh, respectively. The inner radius of the concrete cylinder is:

$$r = r_0\left(\frac{r_0 - t_p}{r_0}\right)^{\eta} \tag{29}$$

where $\eta = k/k_p$.

Eq. (27) is appropriate only under the condition of $R/r = 100$. Otherwise, the thermal diffusivity of concrete should be substituted with an equivalent coefficient α' determined by the following formula:

$$\alpha' = \left(\frac{b}{0.7167}\right)^2 \alpha = 1.947b\alpha \tag{30a}$$

$$b = 0.926\exp\left[-0.0314\left(\frac{R}{r} - 20\right)^{0.48}\right], \quad 20 \le \frac{R}{r} \le 130 \tag{30b}$$

3.2. Equivalent modeling of double-layer heterogeneous cooling pipes

For double-layer staggered heterogeneous cooling pipes in a concrete slab with repetitive horizontal and vertical spacing (Fig. 2), one feasible approach is to subdivide the slab into two regions, where each single material cooling pipe is modeled individually. However, this method is inconvenient because more refinable mesh and corresponding input data are necessary for each subdivision. Therefore, an equivalent modeling method was proposed in this study.

Since the cooling pipes are regularly arranged with equidistance, a rectangular lattice with two heterogeneous cooling pipes can be reasonably extracted as a typical unit cell, as the dashed rectangle illustrated in Fig. 2. Such a lattice configuration forces the solution for the temperature field to be periodic along both the horizontal and vertical directions, which results in equal mean temperature of each unit cell at any time. Obviously, the temperature distribution in the unit cell is not uniform and the effective refrigeration area of each pipe is different as long as the materials of the two pipes differ. However, it still can be approximately divided into two rectangular sublattices where the mean temperature is equal to that of the unit cell, that is, $T_A = T_B = T$.

Table 1
Design conditions for the comparative study of equivalent modeling of double-layer heterogeneous cooling pipes.

Design conditions	Layout of cooling pipes within every lift	Adopted cooling function
Case 1	Iron pipes at the bottom and PVC pipes in the middle	Equivalent modeling approach
Case 2	Iron pipes at the bottom and PVC pipes in the middle	Corresponding cooling function for each sub-layer
Case 3	PVC pipes at the bottom and iron pipes in the middle	Corresponding cooling function for each sub-layer
Case 4	Two-layer iron pipes at the bottom and middle	Cooling function of iron pipes
Case 5	Two-layer PVC pipes at the bottom and middle	Cooling function of PVC pipes

According to Eq. (3), it is equivalent to the condition $\varphi_A = \varphi_B = \varphi$, which yields:

$$\frac{\alpha'_A}{4R_A^2} = \frac{\alpha'_B}{4R_B^2} \tag{31}$$

Thus, with the geometry constraint condition $S_1+S_2 = S_v$, the solution of equivalent cooling function for double-layer heterogeneous cooling pipes can be obtained. This approach was validated through the following example.

A 15-m high concrete column was cast with five lifts at every seven-day interval. The height of every lift was 3 m and the placing temperature was 20 °C. Within every lift, two-layer cooling pipes were located at the bottom and middle of the lift, and the horizontal and vertical spacing of pipes were 1.5 m. The equivalent equation of heat conduction was adopted to model the effect of cooling pipes. The five design conditions listed in Table 1 were used for a comparative study of equivalent modeling of double-layer heterogeneous cooling pipes. For simplicity, the hydration heat of the concrete was not considered and the boundary condition was supposed to be adiabatic. The properties of concrete, cooling water, and pipes are listed in Tables 2 and 3. Inlet temperature of the cooling water was 5 °C and flow was 30 l/min. Every lift was modeled with 6 layers of meshes along its height, as schematically shown in Fig. 3.

The temperature history of the midpoint and two adjacent upper and lower points of the third lift are presented in Fig. 4. Clearly, the cooling effect of the layout of staggered iron and PVC cooling pipes was better than that of double-layer PVC pipes, but weaker than that

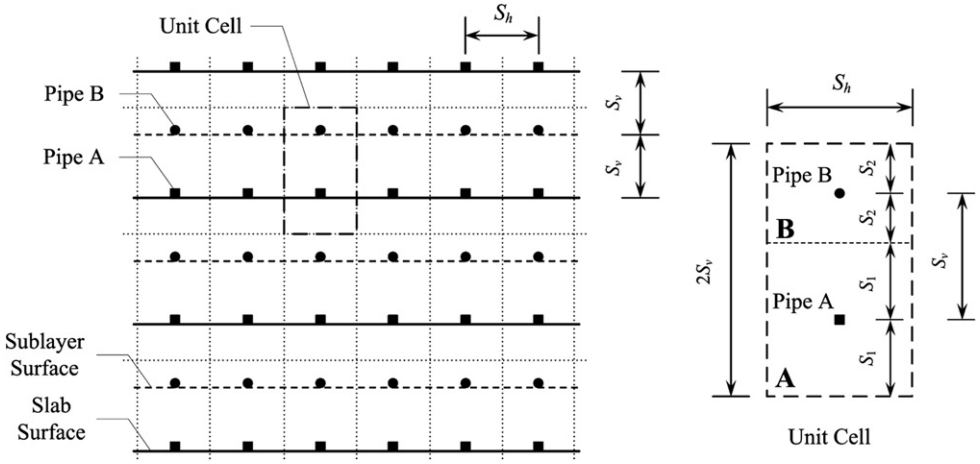

Fig. 2. Schematic diagram of the arrangement of double-layer staggered heterogeneous cooling pipes.

Table 2
Thermal properties of concrete, rock, and cooling water.

Property	Concrete	Rock	Water
Density, ρ (kg/m^3)	2663.0	2670.0	998.5
Thermal conductivity, k (kJ/m·day °C)	184.9	360.0	/
Specific heat, c (kJ/kg °C)	0.86	0.76	4.187
Heat convection coefficient, h (kJ/m^2·day °C)	1005.12	1005.12	/

Table 3
Properties of cooling water pipes.

Property	Iron pipe	PVC pipe
Outer radius, r_0 (mm)	16.75	16.00
Thickness, t_p (mm)	2.75	2.00
Thermal conductivity, k_p (kJ/m·day °C)	3456.00	39.84

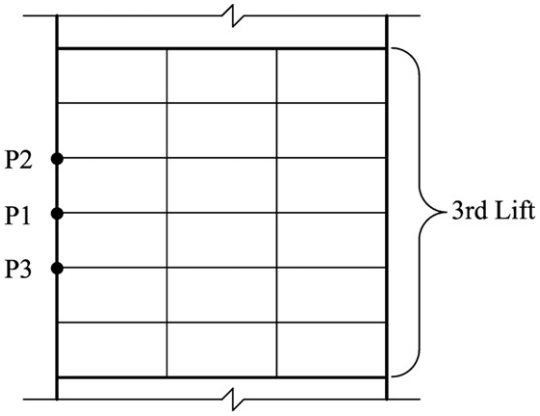

Fig. 3. Schematic diagram of the finite element mesh for a concrete column.

of double-layer iron pipes. By using corresponding cooling function for each sub-layer, the difference was observed between case 2 and 3, where the layout of staggered iron and PVC cooling pipes were opposite to each other. This demonstrates that the sequence of staggered heterogeneous pipes has little influence on the cooling effect. Temperature variation under these two conditions fluctuated around that of case 1, where the equivalent cooling function of double-layer heterogeneous cooling pipes was used. This shows that the equivalent cooling function provides an adequate approximation of the average values for modeling the cooling effect of double-layer staggered heterogeneous cooling pipes.

3.3. Small flow of cooling water

The cooling function $\varphi(t)$ is related to two parameters, k_1 and s, which are fitted by experimental data. The function and its parameters have been verified under common water flow of 10–50 l/min [16], but the applicability under the condition of small flow has not been specified. The equivalent equation of heat conduction is a differential equation of the cooling function. Hence, the mathematical characteristics of the derivative of the cooling function with time should be studied. According to Eq. (27), the derivative of the cooling function $\varphi(t)$ with time yields:

$$\dot{\varphi} = \frac{\partial \varphi(t)}{\partial t} = -k_1 s z^s t^{s-1} \varphi(t) \tag{32}$$

Note that it is only a function of the flow q_w at any time if the properties of concrete, cooling water, and pipes have been determined. Fig. 5 shows the correlation between the derivative of the cooling function and flow under different pipe spacing, 1.0 m × 1.0 m, 1.5 m × 1.5 m and 2.0 m × 2.0 m. There is a turning point at every curve in this figure, which could be referred as the turning point flow q_{m1}. When $q_w \geq q_{m1}$, the derivative of the cooling function is a monotone function decreasing with flow, whereas it is anerraticand incredible function when $q_w < q_{m1}$.

On the other hand, it is well know that the capability of heat transfer in fully developed flow between the laminar and turbulent flow in smooth tubes is quite different. Under most practical conditions, the critical Reynolds number for laminar flow is:

$$\mathrm{Re} = \frac{u_m d}{\nu} = 2300 \tag{33}$$

and the critical laminar flow is:

$$q_{m2} = 575\pi d\nu \tag{34}$$

where $\nu = \mu/\rho_w$ and $d = 2(r_0\text{-}t_p)$. The analysis of heat transfer in tube flow is a very complicated problem that may be solved analytically sometimes, but the solution is considerably complex. For design and engineering purposes, empirical correlations based on experimental studies are usually of greatest practical utility. Supposing that the temperature of mass concrete structures with the cooling pipe system is approximately uniform, the Nusselt number is a constant for a fully developed laminar flow in a smooth circular tube [18]:

$$\mathrm{Nu} = \frac{hd}{k_w} = 3.66 \quad \text{for constant surface temperature} \tag{35}$$

A considerably accurate expression for fully developed flow in smooth tubes is proposed as [21]:

$$\mathrm{Nu} = \frac{(f/8)(\mathrm{Re}-1000)\mathrm{Pr}}{1+12.7(f/8)^{0.5}(\mathrm{Pr}^{2/3}-1)} \begin{pmatrix} 0.5 \leq \mathrm{Pr} \leq 10^6 \\ 2300 \leq \mathrm{Re} \leq 5\times 10^6 \end{pmatrix} \tag{36}$$

$$f = (1.82\log_{10}\mathrm{Re} - 1.64)^{-2} \tag{37}$$

From Eq. (36), the Nusselt number of the critical laminar flow in common cooling pipes, named Nu_{2300}, is larger than the Nusselt number determined by Eq. (35). Hence, a scale factor q_s could be defined as:

$$q_s = 3.66/\mathrm{Nu}_{2300} \tag{38}$$

In other words, the scale factor q_s multiplied by Eq. (36) makes Eq. (35) at the critical laminar flow (Re = 2300). Similar to the Nusselt number, the cooling function and its derivative under laminar flow condition should be modified in the same manner, since they are derived under the condition of turbulent flow. Consequently, the treatment of the derivative of the cooling function of small flow is described as the following cases:

i) $q_{m1} \leq q_{m2}$. The derivative $\dot{\varphi}$ is given by Eq. (32) when $q_w \geq q_{m2}$, and it is modified by the scale factor q_s when $q_w \leq q_{m2}$; that is, $\dot{\varphi} = q_s \dot{\varphi}(q_{m2})$.
ii) $q_{m1} \geq q_{m2}$. The derivative $\dot{\varphi}$ is given by Eq. (32) when $q_w \geq q_{m1}$, and can be fitted by a polynomial function of the flow q_w. The form of the fitting polynomial function is generally $\dot{\varphi} = g(\log_{10} q_w)$. When $q_{m2} \leq q_w \leq q_{m1}$, the derivative $\dot{\varphi}$ can be obtained by extrapolation with this polynomial function. The value of $\dot{\varphi}(q_{m2})$ is also confirmed and the derivative $\dot{\varphi}$ should be modified by the scale factor q_s when $q_w \leq q_{m2}$.

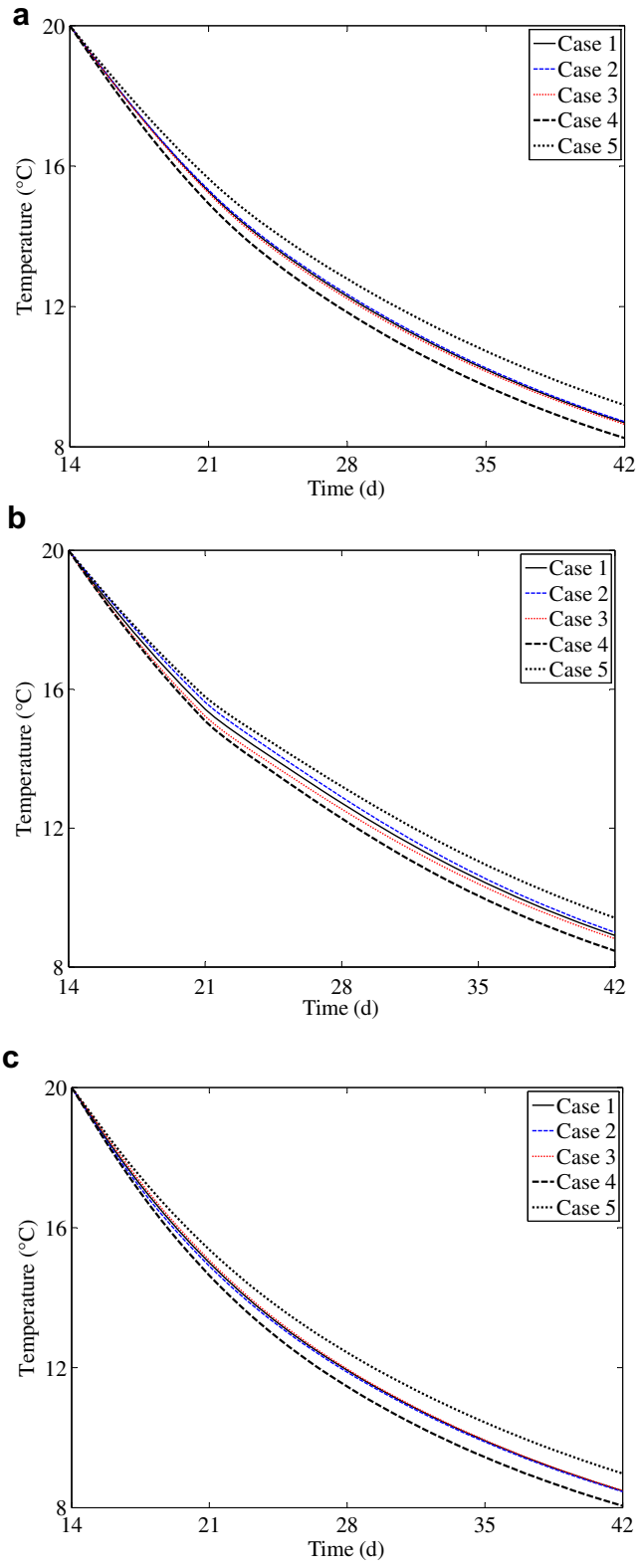

Fig. 4. Temperature variations of the third lift of the concrete column: (a) middle point P1, (b) upper point P2, and (c) lower point P3.

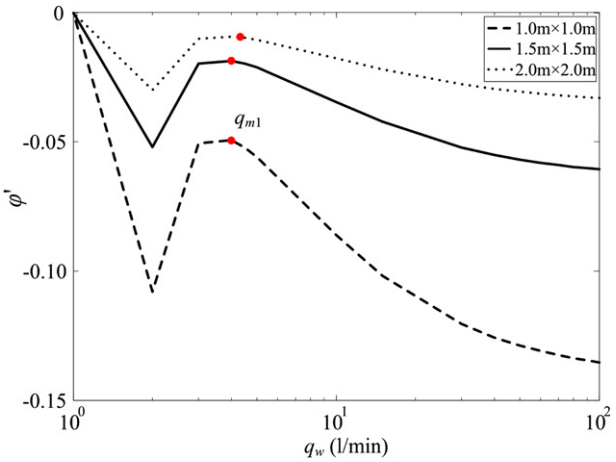

Fig. 5. Correlation between derivative of the cooling function and the flow.

Since the cooling pipe embedded in concrete is long enough, the thermal entrance region where flow is not developed was neglected in the analysis presented above.

4. Adiabatic temperature rise curve of concrete

The hydration heat of concrete is the main heat source in mass concrete structures, and is represented by $\dot{Q}^+$ in Eq. (2). The adiabatic temperature rise model is often used for the simulation of the hydration heat of concrete. One of the most widely used model for ordinary concrete is given by [22,23]:

$$\theta(t) = \theta_0\left(1 - e^{-mt}\right) \tag{39}$$

In current engineering practices, adiabatic temperature rise in concrete is generally determined based on experimental values and then fitted by Eq. (39). Variations in adiabatic temperature rise are almost unmeasured after the age of 28 days because of experiment

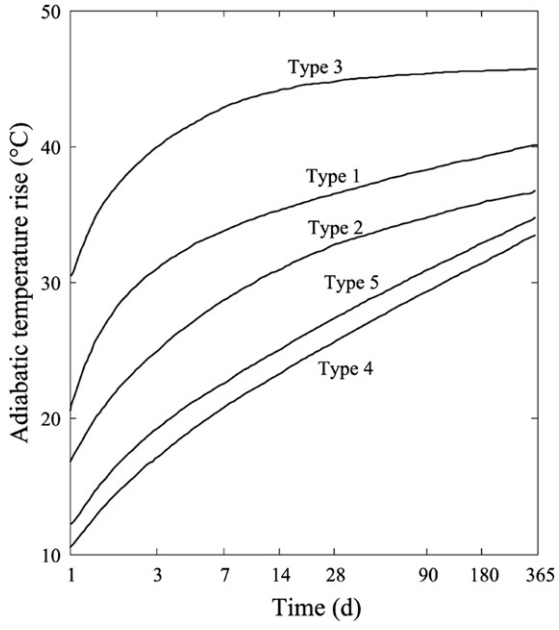

Fig. 6. Adiabatic temperature rise of mass concrete [24].

2010/09/10, 3.0 m, 7 °C	2010/08/20, 3.0 m, 6 °C
2010/08/07, 3.0 m, 6 °C	2010/07/15, 3.0 m, 7 °C
2010/06/17, 3.0 m, 6 °C	2010/05/31, 3.0 m, 6 °C
2010/05/20, 3.0 m, 7 °C	2010/05/14, 3.0 m, 6 °C
2010/05/06, 3.0 m, 7 °C	2010/04/27, 3.0 m, 6 °C
2010/04/18, 3.0 m, 7 °C	2010/04/13, 3.0 m, 6 °C
2010/04/07, 3.0 m, 7 °C	2010/03/31, 3.0 m, 7 °C
2010/03/25, 3.0 m, 9 °C	2010/03/19, 3.0 m, 8 °C
2010/03/11, 3.0 m, 8 °C	2010/03/03, 3.0 m, 9 °C
2010/02/24, 3.0 m, 9 °C	2010/02/07, 3.0m, 10 °C
2010/01/30, 3.0 m, 9 °C	2010/01/10, 3.0 m, 9 °C
2009/12/31, 3.0 m, 9 °C	2009/12/19, 1.5 m, 9 °C
2009/08/23, 1.5 m, 7 °C	2009/08/13, 1.5 m, 7 °C
2009/06/17, 1.5 m, 6 °C	2009/05/25, 1.5 m, 5 °C
2009/05/18, 1.5 m, 6 °C	2009/05/07, 1.5 m, 6 °C

Fig. 7. Construction process of the monolith, indicating the cast date, lift thickness, and placing temperature of each lift.

precision deficiency, which leads to an almost flat trend of the abovementioned model after 28 days. However, the heat of hydration is generated at a considerably slow rate during the later period and the adiabatic temperature increases very slowly. This could be attributed to two possible reasons: i) early hydration degree of mass concrete is lower due to lower placing temperature (about 10 °C or lower); and ii) hydration process of cementitious materials with mineral admixture takes a longer period. Hence, a modified adiabatic temperature rise curve of double exponential function was proposed:

$$\theta(t) = \theta_1\left(1 - e^{-m_1 t}\right) + \theta_2\left(1 - e^{-m_2 t}\right) \tag{40}$$

According to the typical adiabatic temperature generation curves given by ACI 207 [24] (Fig. 6), adiabatic temperature rise

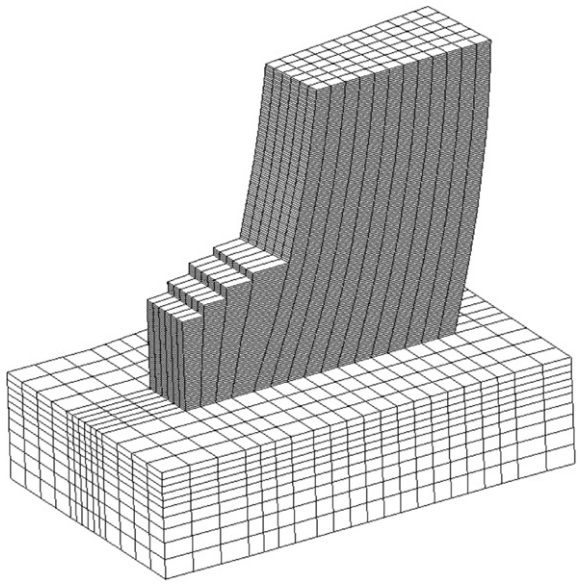

Fig. 9. Schematic diagram of the finite element mesh for the dam monolith.

during day 28–365 for common portland cement (Type I in Fig. 6) and moderate heat of hydration cement (Type II in Fig. 6) exhibited about 10–20 percent of the temperature rise at day 28. Consequently, adiabatic temperature rise curve of concrete can be fitted with Eq. (40) based on the experimental data and empirical assumptions of $\theta_{90} = \alpha_1\theta_{28}$ and $\theta_{365} = \alpha_2\theta_{28}$, where θ_{28}, θ_{90} and θ_{365} are adiabatic temperature rise at day 28, 90, and 365, respectively.

5. Formulation of outlet temperature of cooling water

Outlet temperature of cooling water is generally higher than inlet temperature because the hydration heat of concrete is partly absorbed by cooling water. To calculate the outlet temperature of cooling water at any time, the energy conservation principle (i.e. the heat supplied to pipes is equal to the heat absorbed by the flowing water) is introduced.

The heat flux supplied to pipes per unit volume $\dot{Q}^-$ is derived from Eq. (2) and (6) as:

$$\dot{Q}^- = \dot{Q} - \dot{Q}^+ = \rho c\left[(T_0 - T_w)\frac{\partial\varphi(t)}{\partial t} + \theta_0\frac{\partial\psi(t)}{\partial t} - \frac{\partial\theta(t)}{\partial t}\right] \tag{41}$$

The heat absorbed by cooling water per unit time is:

$$q_{\text{cool}} = \rho_w c_w q_w (T_{\text{w-out}} - T_{\text{w-in}}) \tag{42}$$

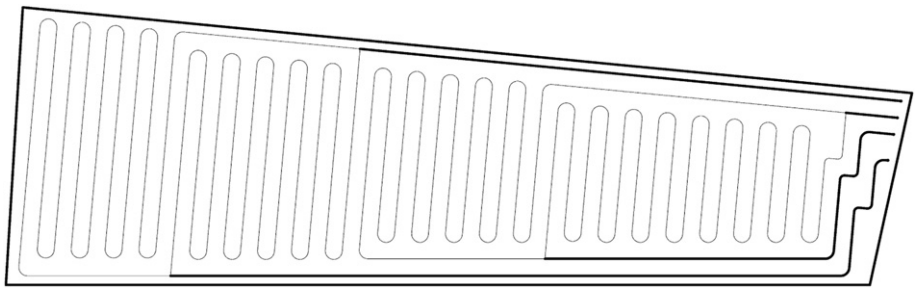

Fig. 8. Typical layout of a pipe loop in a lift.

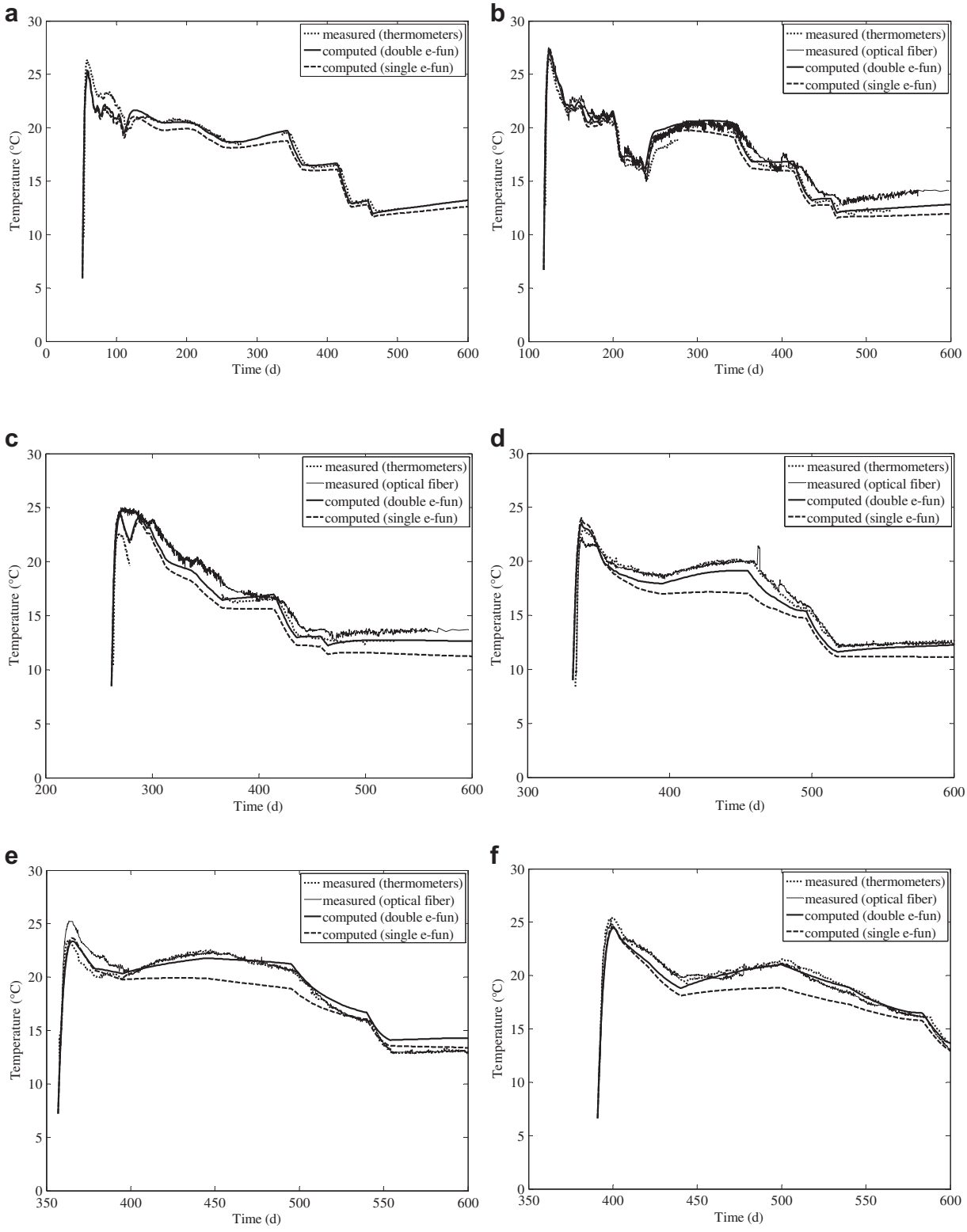

Fig. 10. Temperature variations of concrete in typical slabs: (a) Fourth lift, (b) Sixth lift, (c) Ninth lift, (d) Sixteenth lift, (e) Twentieth lift, and (f) Twenty-fourth lift.

Since variations in kinetics and potential energy of cooling water are extremely small, the energy conservation principle yields:

$$q_{\text{cool}} + \int_V \dot{Q}^- [\mathbf{N}]^T dV = 0 \tag{43}$$

Hence, outlet temperature can be obtained as:

$$T_{\text{w-out}} = \frac{\rho c \int_V \left[(T_0 - T_{\text{w-in}}) \frac{\partial \varphi(t)}{\partial t} + \theta_0 \frac{\partial \psi(t)}{\partial t} - \frac{\partial \theta(t)}{\partial t} \right] [\mathbf{N}]^T dV}{\rho_w c_w q_w} + T_{\text{w-in}} \tag{44}$$

6. Case study

6.1. Modeling of an arch dam monolith

A 286-m high parabolic double-curvature arch dam under construction is located in Southwest China at an altitude of 610 m above sea level (level of crest). The dam consists of 31 monoliths for a total crest length of 680 m. The crown cantilever has a crest thickness of 14 m and a base thickness of 60 m. One of the monoliths on the riverbed, which was started on May 7, 2009, was selected for the thermal analysis in this study. To that date, stage number 30 had been completed and a height of 79.5 m had been achieved. The progress of monolith construction to the 30th lift with respect to time is shown in Fig. 7.

From 1st to 7th lift, there was only one layer of iron cooling pipes arranged on the bottom of the slab. From the 8th to 18th lift, there was a double-layer of heterogeneous cooling pipes, with iron pipes at the bottom and PVC pipes at the central elevation. Otherwise, there was a double-layer of PVC pipes in a slab. The typical layout of a pipe loop is shown in Fig. 8, with horizontal and vertical spacing of 1.5 m. Thermometers and distributed optical fiber temperature system were embedded in every lift away from the pipes at a height of about 0.5–1.0 m.

Fig. 9 shows the finite element mesh of the monolith. The thickness of an element for the dam body was 0.5 m. When a fresh concrete slab was poured, the corresponding elements in the finite element model were immediately activated and included in the solution.

6.2. Boundary conditions and initial conditions

The monolith gradually rose with the progress of construction. Increasing upstream and downstream surfaces of poured concrete slabs and the top surface of the latest slab were assumed to be directly exposed to the environment, where heat transfer by convention and radiation occurred. Daily mean air temperature at the dam site was used in this analysis. The effect of solar radiation was simply taken into account through increasing ambient temperature by 2 °C [8].

Since the construction of the selected monolith was always behind that of adjacent monoliths, the boundary condition of both sides was assumed to be adiabatic.

Supposing that the initial temperatures of all the nodes of the foundation were all equal to annual mean air temperature, heat transfer between the environment and the foundation over a year was analyzed. Thus, the temperature distribution in the foundation was obtained.

6.3. Properties of materials

The thermal properties of placed concrete and rock are summarized in Table 2. In order to investigate the effect of the cooling pipe, the thermal properties of cooling water and cooling pipes (Table 2 and Table 3, respectively) were used. During pipe cooling, inlet temperatures varied within the range of 8–20 °C, whereas the flow of cooling water was within 1–50 l/min. Daily mean values of inlet temperature and flow were used in the numerical analysis. The scale factor q_s when there was small flow of cooling water was 0.21.

Fitting analysis with Eq. (39) based on experimental data yielded parameters $\theta_0 = 26.0$ °C and $m = 0.25$ day^{-1}. Assuming $\theta_{90} = \alpha_1\theta_{28}$ and $\theta_{365} = \alpha_2\theta_{28}$, where α_1 and α_2 were 1.1 and 1.2, respectively, the fitting analysis with Eq. (40) resulted in $\theta_1 = 25.3$ °C, $\theta_2 = 6.2$ °C, $m_1 = 0.26$ day^{-1}, and $m_2 = 0.0085$ day^{-1}.

6.4. Results and discussions

The comparison of temperature histories of concrete between calculated results and actual measured temperature from thermometers and optical fibers in the six typical slabs are presented in Fig. 10. Overall calculated results obtained from the procedure developed in this study were in good agreement with the measured data. Maximum peak temperatures at early age were accurately captured by the developed code in most lifts, and the discrepancy between calculated and measured data did not exceed 1 °C.

The trend of predicted temperature variations in slabs where double-layer heterogeneous cooling pipes were used coincided with the actual trends observed (Fig. 10(c) and (d)), thereby proving the rationality of equivalent modeling of double-layer heterogeneous cooling pipes. Calculated results were slightly lower than measured data most of the time because the equivalent modeling approach did not include the effect of sequence of staggered heterogeneous pipes, as already explained earlier.

Obviously, temperature recovery in concrete was observed at late ages (at least two months after casting), when the slab has been covered by newer lifts. The internal temperature of the slab was almost independent of environmental influence. Consequently, the phenomenon of temperature recovery was attributed to internal heat generation by concrete. Fig. 10 shows that temperature recovery was reproduced perfectly using the adiabatic temperature rise curve of a double exponential function to consider heat hydration of other cementitious materials at late age. Otherwise, conventional adiabatic temperature rise model with a single exponential function had worse performance.

The 20th lift, which experienced a long time of laminar flow, was selected for the investigation of the effect of scale factor q_s for small flow. We considered three situations: no effect, modified effect, and full effect, corresponding to q_s of 0.0, 0.21, and 1.0 respectively. Fig. 11 illustrates the comparison of temperature variations of concrete. Predicted temperature considering the modified effect with $q_s = 0.21$ was concurred with measured data, whereas that of no effect was higher and that of full effect was lower than actual values. Thus, modification of cooling effect under laminar flow condition is necessary, and the approach presented here is appropriate.

Variations in outlet and inlet temperature of cooling pipes and in flow of cooling water in six typical slabs are presented in Fig. 12. Results indicate that the temperature increase of cooling water was

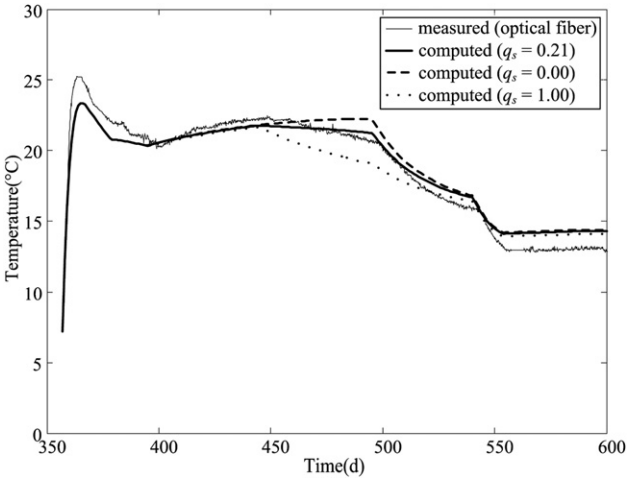

Fig. 11. Comparison of the effects of scale factor q_s for small flow.

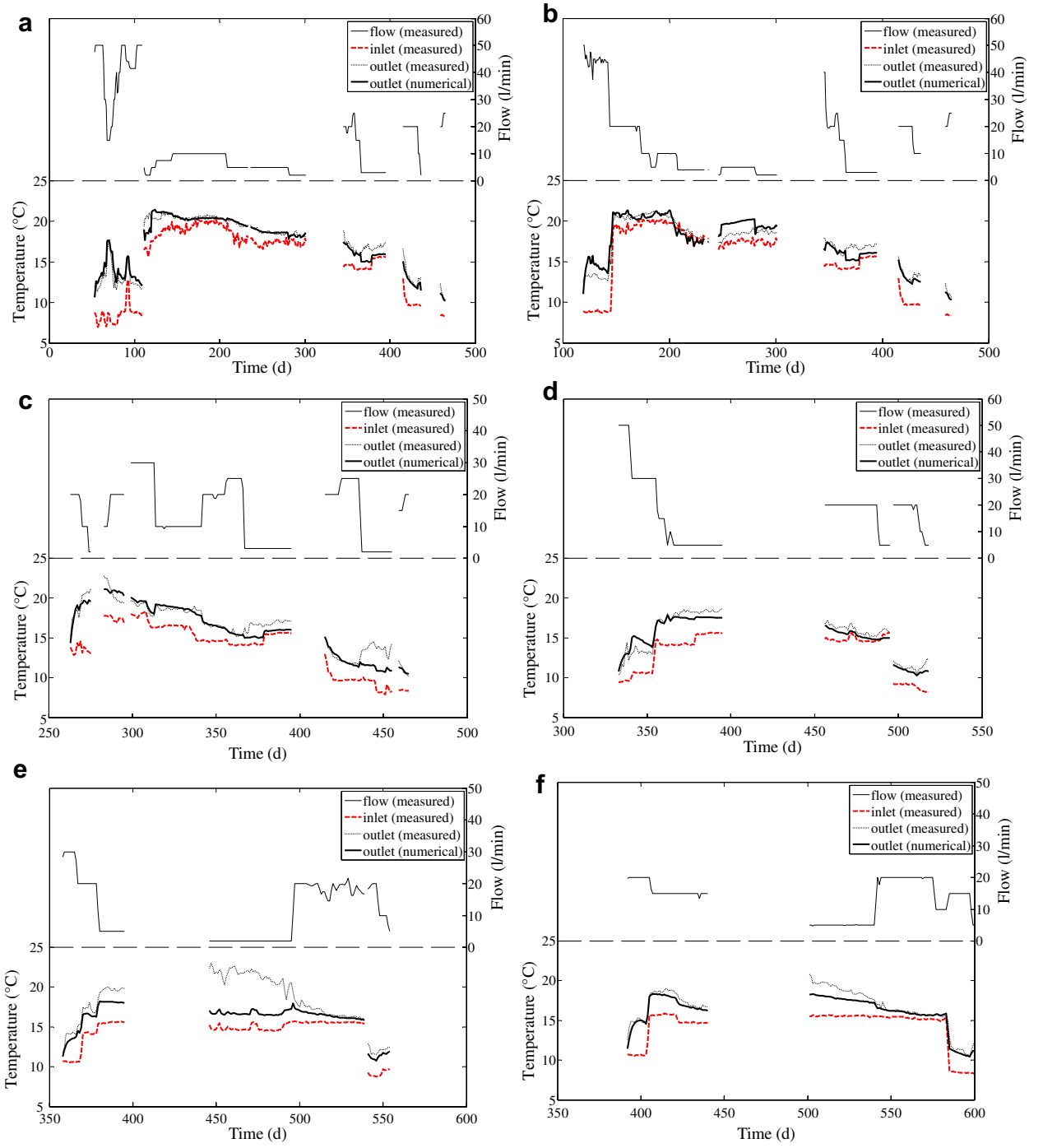

Fig. 12. Variations in outlet and inlet temperature of cooling pipes and in flow of cooling water in typical slabs: (a) Fourth lift, (b) Sixth lift, (c) Ninth lift, (d) Sixteenth lift, (e) Twentieth lift, and (f) Twenty-fourth lift.

well estimated, especially during the period of large flow. Lower calculation precision during the period of small flow may be attributed mainly to error amplification. If the error of concrete temperature in a step time Δt is δT and induced heat error was only absorbed by cooling water, error estimation of outlet water temperature could be derived as $\delta T_{\text{w-out}} = \rho c V \delta T / \rho_w c_w q_w \Delta t$, according to the energy conservation principle. This indicates that error estimation of outlet water temperature is inversely proportional to the flow. Thus, error of outlet temperature increases with smaller water flow.

7. Conclusion

In this study, we developed a 3D finite element program for thermal analysis of mass concrete embedded with double-layer staggered heterogeneous cooling water pipes based on the equivalent equation of heat conduction including hydration heat of concrete and the effect of cooling pipe system. The cooling function for the effect of double-layer staggered heterogeneous cooling pipes in a concrete slab was derived from the principle of equivalent cooling.

According to forced-convention heat transfer of internal flow, the cooling effect under laminar flow condition using equivalent heat conduction equation was proposed to be modified by a scale factor q_s. Monotonicity of the derivative of the cooling function with time was discussed in detail to improve the applicability and precision of the equivalent heat conduction equation under small flow. Considering heat hydration of concrete at late age, a double exponential function was presented to fit the adiabatic temperature rise curve of concrete. Once temperature variation of concrete was obtained, the energy conservation principle was implemented to estimate the outlet temperature of cooling water.

We verified the reliability, precision and efficiency of the developed 3D finite element program by comparing the calculated results and actual measured temperature of a dam monolith with a cooling pipe system. Outlet temperature of cooling water was efficiently obtained by the model. Findings of this study demonstrate that the developed program can be applied in the thermal analysis of mass concrete structures with an embedded pipe cooling system during the design and construction phase.

Acknowledgements

This research was supported by National Natural Science Foundation of China (No.50539020).

References

[1] A.M. Neville, Properties of Concrete. Longman, Essex, England, 1995.
[2] D.C. Lawrence, Physiochemical and mechanical properties of portland cement. in: P.C. Hewlett (Ed.), LEA'S Chemistry of Cement Concrete. Butterworth and Heinemann, Oxford, England, 1998, pp. 343–420.
[3] American Concrete Institute, Cooling and Insulating Systems for Mass Concrete (ACI 207.4R-05) (2005).
[4] US Bureau of Reclamation. The Story of Hoover Dam. http://www.usbr.gov/lc/hooverdam/History/essays/concrete.html.
[5] G. Hauser, C. Kempkes, B.W. Olesen, Computer simulation of hydronic heating/cooling system with embedded pipes, ASHRAE Transactions 106 (2000) 702–710.
[6] R.E. Glover, Cooling of Concrete Dams. Final reports for Boulder Canyon Project. United States Department of the Interior, Bureau of Reclamation, Denver, 1949.
[7] B.F. Zhu, Calculation of temperatures in mass concrete with internal source of heat, cooled by embedded pipes, Chinese Journal of Hydraulic Engineering 4 (1957) 87–106 (in Chinese).
[8] The Ministry of Water Resources of the People's Republic of China, Design Specification for Concrete Arch Dam. China WaterPower Press, Beijing, 2003, (in Chinese).
[9] C. Liu, Temperature field of mass concrete in pipe lattice, Journal of Materials in Civil Engineering 16 (5) (2004) 427–432.
[10] J.P.F. Charpin, T.G. Myers, A.D. Fitt, N.D. Fowkes, D.P. Mason, Piped water cooling of concrete dams, in: Proceedings of the 1st South African Mathematics in Industry Study Group. Univ. of the Witwatersrand, Johannesburg, South Africa, 2004, pp. 69–86.
[11] T.G. Myers, N.D. Fowkes, Y. Ballim, Modeling the cooling of concrete by piped water, Journal of Engineering Mechanics 135 (12) (2009) 1375–1383.
[12] B.F. Zhu, J.B. Cai, Finite element analysis of effect of pipe cooling in concrete dams, Journal of Construction Engineering and Management 115 (4) (1989) 487–498.
[13] J.K. Kim, K.H. Kim, J.K. Yang, Thermal analysis of hydration heat in concrete structures with pipe-cooling system, Computers and Structures 79 (2) (2001) 163–171.
[14] H. Kawaraba, T. Kanokogi, T. Tanabe, Development of the FEM program for the analysis of pipe cooling effects on the thermal stress of massive concrete, Transaction of Japanese Concrete Institute 8 (1986) 45–48 (in Japanese).
[15] M.S. Roberta, Finite Element Modeling of Cooling Coil Effects in Mass Concrete Systems (final report), ERDC/ITL TR-01–3. US Army Corps of Engineers, St. Louis, 2001.
[16] B.F. Zhu, Equivalent equation of heat conduction in mass concrete considering the effect of pipe cooling, Chinese Journal of Hydraulic Engineering 3 (1991) 28–34 (in Chinese).
[17] H.W. Xie, Y.L. Chen, Influence of the different pipe cooling scheme on temperature distribution in RCC arch dams, Communication in Numerical Methods in Engineering 21 (12) (2005) 769–778.
[18] Y.A. Cengel, Heat and Mass Transfer: A Practical Approach, third ed. McGraw-Hill, Boston, 2007.
[19] B.F. Zhu, Effect of cooling by water flowing in nonmetal pipes embedded in mass concrete, Journal of Construction Engineering and Management 125 (1) (1997) 61–68.
[20] A. Stucky, M. Derron, Problèmes thermiques posés par la construction des barrages-réservoirs EPFL publication no 38. Editions Sciences and Techique, Paul Feissly éditeur, Lausanne, 1957.
[21] Adrian Bejan, Allan D. Kraus, Heat Transfer Handbook. John Wiley & Sons, Inc., Hoboken, New Jersey, 2003.
[22] Japan Concrete Institute, Standard Specifications for Design and Construction of Concrete Structures, Part 2 (Construction) Tokyo (1986).
[23] M. Ishikawa, Thermal stress analysis of a concrete dam, Computers and Structures 40 (2) (1991) 347–352.
[24] American Concrete Institute, Mass Concrete (ACI 207.1R-96) (1996).